Received: 29 September 2021 | Revised: 16 December 2021 | Accepted: 4 January 2022

DOI: 10.1111/jam.15443

Journal of Applied Microbiology sfam

ORIGINAL ARTICLE

Structure and functional capacity of a benzene-mineralizing, nitrate-reducing microbial community

Samuel C. Eziuzor[1] | **Felipe B. Corrêa**[2] | **Shuchan Peng**[1,3] | **Júnia Schultz**[2,4,5] | **Sabine Kleinsteuber**[2] | **Ulisses N. da Rocha**[2] | **Lorenz Adrian**[6,7] | **Carsten Vogt**[1]

[1]Department of Isotope Biogeochemistry, Helmholtz-Centre for Environmental Research – UFZ, Leipzig, Germany

[2]Department of Environmental Microbiology, Helmholtz-Centre for Environmental Research – UFZ, Leipzig, Germany

[3]Department of Environmental Science, Chongqing University, Chongqing, China

[4]Departamento de Microbiologia Geral, Universidade Federal do Rio de Janeiro, Rio de Janeiro, Rio de Janeiro, Brazil

[5]Biological and Environmental Science and Engineering Division, King Abdullah University of Science and Technology (KAUST), Thuwal, Saudi Arabia

[6]Department of Environmental Biotechnology, Helmholtz Centre for Environmental Research – UFZ, Leipzig, Germany

[7]Geobiotechnology, Technische Universität Berlin, Berlin, Germany

Correspondence
Carsten Vogt, Department of Isotope Biogeochemistry, Helmholtz-Centre for Environmental Research – UFZ, Leipzig, Germany.
Email: carsten.vogt@ufz.de

Funding information
Deutscher Akademischer Austauschdienst; Helmholtz Association, Grant/Award Number: VH-NG-1248

Abstract

Aims: How benzene is metabolized by microbes under anoxic conditions is not fully understood. Here, we studied the degradation pathways in a benzene-mineralizing, nitrate-reducing enrichment culture.

Methods and results: Benzene mineralization was dependent on the presence of nitrate and correlated to the enrichment of a *Peptococcaceae* phylotype only distantly related to known anaerobic benzene degraders of this family. Its relative abundance decreased after benzene mineralization had terminated, while other abundant taxa—*Ignavibacteriaceae*, *Rhodanobacteraceae* and *Brocadiaceae*—slightly increased. Generally, the microbial community remained diverse despite the amendment of benzene as single organic carbon source, suggesting complex trophic interactions between different functional groups. A subunit of the putative anaerobic benzene carboxylase previously detected in *Peptococcaceae* was identified by metaproteomic analysis suggesting that benzene was activated by carboxylation. Detection of proteins involved in anaerobic ammonium oxidation (anammox) indicates that benzene mineralization was accompanied by anammox, facilitated by nitrite accumulation and the presence of ammonium in the growth medium.

Conclusions: The results suggest that benzene was activated by carboxylation and further assimilated by a novel *Peptococcaceae* phylotype.

Significance and impact of the study: The results confirm the hypothesis that *Peptococcaceae* are important anaerobic benzene degraders.

KEYWORDS

anaerobic benzene degradation, anammox bacteria, dissimilatory nitrate reduction, *Peptococcaceae*, putative anaerobic benzene carboxylase

INTRODUCTION

Benzene is part of petroleum and gasoline and can contaminate soil, sediment and aquifers during oil extraction, production and related industrial activities (Landon & Belitz, 2012). It is a highly toxic volatile aromatic compound and a known carcinogen (Bayliss et al., 1997; European Chemicals Agency, 2018). The molecule is chemically very stable due to its aromatic ring system (π-electron system) and the absence of any reactive substituent. Genes and enzymes for aerobic benzene activation and degradation through catechol intermediates are well known (Díaz et al., 2013; Weelink et al., 2010). Under anoxic conditions, benzene is slowly metabolized by microbial consortia under different redox conditions; only a few pure cultures have been thus far described that are capable of anaerobic benzene mineralization (Coates et al., 2001; Holmes et al., 2011; Kasai et al., 2006). It is not fully understood how benzene is activated in the absence of oxygen. Metabolite studies with different cultures indicated three potential activating mechanisms: hydroxylation to phenol, methylation to toluene or carboxylation to benzoate (summarized by Vogt et al., 2011). Formed phenol, toluene or benzoate could be transformed to the central intermediate benzoyl-CoA by known pathways (Fuchs, 2008). The enzymatic steps upon dearomatization of benzoyl-CoA, subsequent ring cleavage and subsequent reactions leading to tricarboxylic acid intermediates are also well studied (Boll et al., 2014).

Indications for hydroxylation as activation step were found in experiments with the iron reducer *Geobacter metallireducens* by the production of ^{18}O-labelled phenol in $H_2{}^{18}O$-labelled water and halting benzene degradation by knocking out phenol degradation genes (Zhang et al., 2013); a similar observation of ^{18}O-labelled phenol produced in ^{18}O-labelled water was formerly reported for a methanogenic benzene-degrading enrichment culture (Vogel & Gribič-Galič, 1986). Furthermore, another methanogenic mixed culture was reported to produce $^{13}C_6$-phenol upon amendment of $^{13}C_6$-benzene (Ulrich et al., 2005).

Holmes et al. (2011) provided transcriptomic evidence of benzene carboxylation as an initial step in the hyperthermophilic archaeon *Ferroglobus placidus*, which employed a putative UbiD-related carboxylase under Fe(lll)-reducing conditions. Using a highly enriched iron-reducing culture (BF) composed mainly of organisms related to *Peptococcaceae*, a putative benzene degradation gene cluster encoding carboxylase-related enzymes was found to be expressed during growth with benzene; the authors postulated that the initial activation reaction in BF was a direct carboxylation of benzene to benzoate catalysed by a putative anaerobic benzene carboxylase named Abc composed of two subunits, AbcA and AbcD (Laban et al., 2010). Similar observations were made in nitrate-reducing benzene-degrading enrichment cultures, in which *Peptococcaceae* were identified as essentially involved in the initial transformation of benzene, and the putative anaerobic benzene carboxylase encoding genes *abcA* and *abcD* were only transcribed upon amendment of benzene (Atashgahi et al., 2018; Luo et al., 2014; Melkonian et al., 2021). A recent study points to the importance of organisms belonging to the genus *Thermincola* within the *Peptococcaceae* as primary benzene degraders under nitrate-reducing conditions (Toth et al., 2021).

Notably, the concurrent transcription of genes encoding enzymes catalysing oxygen-dependent benzene hydroxylation was also observed during benzene degradation under nitrate-reducing conditions (Atashgahi et al., 2018; Melkonian et al., 2021), suggesting either oxygen contamination or the presence of molecular oxygen possibly formed via nitric oxide dismutase as proposed for methane or alkane oxidizers under nitrate-reducing conditions (Ettwig et al., 2010; Zedelius et al., 2011).

Syntrophic interactions and diverse metabolic processes in benzene-degrading enrichment cultures have been commonly described (Rakoczy et al., 2011; van der Zaan et al., 2012). Recently, it was revealed that anaerobic ammonium oxidation (anammox) by organisms affiliated to *Candidatus* Brocadia fulgida and *Candidatus* Kuenenia accelerated benzene degradation under nitrate-reducing conditions (Han et al., 2020; Peng et al., 2017).

The goal of the present study was to elucidate the key players and degradation pathway of a benzene-mineralizing nitrate-reducing microbial community enriched from a benzene-contaminated megasite in Zeitz, Germany. A previous study described benzene degradation characteristics of this community, which was mainly composed of *Betaproteobacteria*, *Ignavibacteria* and *Anaerolineae*, with *Azoarcus* and a phylotype related to clone Dok59 (*Rhodocyclaceae*) as the dominant genera (Keller et al., 2017). Here, we carried out a metaproteome analysis during a time-course benzene mineralization experiment to characterize the structure and functional capacity of the microbial community.

MATERIALS AND METHODS

Chemicals

Chemicals were purchased from Fluka, Merck, Roth, and Sigma-Aldrich in p.a. quality if not otherwise stated. Benzene-$^{13}C_6$ was purchased from Sigma-Aldrich with an isotopic purity of 99 atom % ^{13}C.

Microcosm setup and sampling

A mineralization experiment was set up with a benzene-mineralizing nitrate-reducing culture. The inoculum was taken from an on-site column system containing coarse sand and percolated with nitrate-amended groundwater from a benzene-contaminated aquifer and maintained for several years in the laboratory under nitrate-reducing conditions (Keller et al., 2017). Each microcosm was setup in 240 ml sterile serum bottles (Glasgerätebau Ochs, Bovenden-Lenglern, Germany) containing 60 g wet weight of coarse sand inoculum filled with anoxic mineral medium composed and prepared according to Vogt et al. (2007) with the exception that sulfate (20 mM) was replaced by nitrate (10 mM), and leaving approximately 5 ml headspace. Notably, the medium contained 7.5 mM ammonium chloride, allowing anammox bacteria to develop. All microcosms were set up in an anaerobic glove box (Coy Laboratory Products Inc.) containing a gas atmosphere of 97% N_2 and approximately 3% H_2. ^{13}C-labelled (25 atom% $^{13}C_6$) and unlabelled benzene stock solutions were prepared in anoxic 2,2,4,4,6,8,8-heptamethylnonane (HMN) as a carrier phase containing 1% (v/v) benzene, and added to the microcosmsthat a theoretical concentration of 1.725 mM benzene in the water-HMN two phase system resulted. Nevertheless, the main part of the benzene was dissolved in the HMN carrier phase thus providing a stock amount of benzene in the microcosm allowing substantial growth of benzene assimilating organisms by concurrently avoiding potentially toxic benzene concentrations in the aqueous phase. Labelled benzene stock solution was prepared by mixing 25% (vol) fully labelled $^{13}C_6$-benzene and 75% (vol) unlabelled benzene. Fifteen microcosms were prepared with mineral medium containing 10 mM nitrate and spiked with 3 ml ^{13}C-labelled benzene-HMN solution while two additional nitrate-amended microcosms were spiked with 3 ml unlabelled benzene-HMN solution. Additional controls included: (i) nitrate-free triplicate microcosms spiked only with 3 ml labelled benzene-HMN solution (nitrate-free control), (ii) nitrate-amended (10 mM) triplicate microcosms spiked with benzene-free HMN (benzene-free control), and (iii) triplicate microcosms amended with nitrate (10 mM) and labelled benzene-HMN autoclaved three times on consecutive days as abiotic control. All microcosms were sealed with gas-tight inert Teflon-coated butyl rubber stoppers (ESWE Analysentechnik, Gera, Germany). The microcosms were incubated statically for 124 days at room temperature in the dark. Liquid samples for chemical analyses and gaseous samples for isotope analyses were taken with sterile syringes previously flushed with nitrogen.

Samples for proteomic and biodiversity analyses were obtained by sacrificing whole microcosms of the ^{13}C-labelled benzene setups based on their $^{13}CO_2$ formation in biological triplicates at five different time points on day 0, day 70, day 76, day 96 and day 124 (summarized in Table S1). Microcosms amended with unlabelled benzene and control microcosms were sacrificed after 124 days of incubation. Separate liquid and solid samples were taken from each microcosm except for day 0, on which liquid and solid samples were taken as a single sample. From the other microcosms, 5 ml of liquid and 5 ml solid material were filled directly into Lysing Matrix E 15 ml tubes (MP Biomedicals), respectively, which were immediately stored at −80°C until further proceeding (see below). For proteomic analysis, 50 ml of liquid and approximately 20 g wet weight of solid material were filled into 50 ml conical tubes (Eppendorf) respectively. The solid samples were sonicated in deionized water using a Sonorex Super RK 103 H ultrasonic bath (Bandelin) at a frequency of 20 kHz for 10 min to detach the cells from the coarse sand, a procedure which was repeated three times. The cell suspensions were combined and centrifuged at 17,700 × g at 4°C for 10 min to obtain pellets as well as for the liquid samples. The pellets were immediately stored at −80°C until protein extraction.

Additionally, a separate experiment was setup to analyse the presence of genes encoding nitric oxide dismutase (*nod* genes) and internally produced oxygen as described above for the mineralization setup except that triplicate microcosms were prepared using 120 ml serum bottles amended with nitrate (10 mM) and either non-diluted ^{13}C-labelled benzene (99 atom% $^{13}C_6$) or unlabelled benzene. In this experiment, benzene was spiked directly without using a HMN phase to a final concentration of 0.3 mM using a microliter gas-tight syringe (Hamilton). One microcosms amended with ^{13}C-labelled benzene and nitrate was autoclaved (20 min, 121°C) and served as abiotic control. The bottles were opened at the end of the experiment for DNA extraction and subsequent PCR analysis for *nod* genes.

Chemical and physiochemical analyses

Nitrite concentrations were spectrophotometrically determined according to Raihan et al. (1997). A volume of 125 µl nitrite determination reagent (10 g L^{-1} sulfanilamide, 0.5 g L^{-1} napthylethylenediamine dihydrochloride dissolved in 10% H_3PO_4) was added to 500 µl sample, vortexed and incubated in the dark for 10 min. Absorbance was measured at 540 nm against a standard consisting of 125 µl determination reagent mixed with 500 µl distilled

water. Quantification was done with an external standard calibration.

The carbon isotope ratio of CO_2 ($\delta^{13}CO_2$) was determined using a gas chromatograph-isotope ratio mass spectrometer as described elsewhere (Herrmann et al., 2010). Each sample was measured in at least three replicates; the reproducibility of $\delta^{13}C$ values was always better than 0.5‰. Carbon isotope ratios were expressed in the delta notation in per mil ($\delta^{13}C$/‰) units relative to the Vienna Pee Dee Belemite (VPDB) according to the following equation (Coplen, 2011):

$$\delta^{13}C_{sample}[‰] = \left(\frac{R_{sample}}{R_{reference}} - 1\right),$$

where R_{sample} and $R_{reference}$ are the ratios of the heavy isotope to the light isotope ($^{13}C/^{12}C$) in the sample and in the standard (VPDB) respectively.

Putative internally produced oxygen in the microcosms was measured using PC-controlled optical oxygen sensors using PreSens Measurement Studio 2 software (PreSens Precision Sensing GmbH). Two non-invasive optical precalibrated oxygen sensor spots were fixed at the inner surface of glass serum bottles representing the liquid phase and headspace after microcosm preparation. Oxygen was measured from outside the bottle, through the glass wall using the polymer optical fibre. The applied sensor spot PSt6 measures oxygen in the range of 0%–5% in the gaseous phase or 0–2 mg L^{-1} in the liquid phase with a detection limit of 0.002% oxygen or 1 ppb and a temperature measurement range of 0–50°C. Oxygen measurements were carried out daily throughout the experiment.

Amplicon and metagenome sequencing

Total DNA was extracted using a cetyl trimethylammonium bromide/phenol-chloroform approach according to Rajeev et al. (2013). DNA quantification was done using a Qubit fluorometer and the Qubit dsDNA BR assay kit (Thermo Fisher Scientific GmbH). DNA was stored at −80°C until further use. Microbial community composition was analysed by paired-end sequencing of 16S rRNA amplicons on the Illumina MiSeq platform using the MiSeq Reagent Kit v3 (2 × 300 bp). The V3–V4 regions of the 16S rRNA genes were amplified using the primers according to Klindworth et al. (2013). Resolution of amplicon sequence variants (ASVs) and taxonomic assignment were done using the QIIME 2 version 2018.11.0 (Bolyen et al., 2019). ASVs were resolved using the DADA 2 plugin (Callahan et al., 2016), where sequencing reads were truncated and quality-checked with parameters --p-trunc-len-f = 276, --p-trunc-len-r = 216 and --p-max-ee = 8. Primer sequences were trimmed from the reads with parameters --p-trim-left-f = 18 and --p-trim-left-r = 22. The taxonomic assignment of ASVs was performed using SILVA version 132 (Quast et al., 2013) as a reference database. Relative abundances were calculated after removing low abundant ASVs (<0.01 in the whole dataset) and plots were generated using the Phyloseq R package (McMurdie & Holmes, 2013). Fourteen metagenome samples gained from different sacrificed microcosm along the time course of the experiment (Table S3) were sequenced on the Illumina NextSeq 500™ system at StarSEQ® GmbH to produce a custom database of predicted genes for protein annotation. Whole genome sequencing yielded approximately 30 million paired-end reads per library with an average read length of 150 nucleotides. The metagenome data comprised a total of 141,368,768,510 nucleotides.

Protein mass spectrometry

Cells obtained from liquid and solid samples were disrupted by three cycles of freezing in liquid nitrogen and thawing at 40°C and 750 rpm for 60 s. The disrupted cells were sonicated for 30 s at 50% intensity in an ultrasonic bath and centrifuged afterwards at 6700 × g for 30 min. An internal standard of 2 µl of *Staphylococcus aureus* glyceraldehyde 3-phosphate dehydrogenase was added. Disulphide bridges were reduced with 1 M dithiothreitol to sulfhydryl groups. Then, cysteine residues were alkylated by incubation with 100 mM iodoacetamide in 50 mM ammonium bicarbonate for 30 min at room temperature in the dark. Subsequent digestion was performed by adding 0.1 µg of porcine trypsin (Proteomic Sequencing Grade) and incubating at 37°C overnight. The digestion was stopped by adding 1 µl of 100% formic acid using a 1 µl fixed volume pipette with a glass tip and centrifuged at 11,400 × g to precipitate undigested proteins while the supernatant containing the digested proteins was transferred into a new tube. The volume of the supernatant was reduced to 10–20 µl in a vacuum centrifuge. The peptide samples were desalted using ZipTip-µC18 material (Merck Millipore) prior to analysis by liquid chromatography (HPLC Ultimate 3000 nanoRSLC; Thermo Scientific) coupled via a TriVersa NanoMate (Advion, Ltd.) to an Orbitrap Fusion mass spectrometer (Thermo Scientific) as described previously (Türkowsky et al., 2019). Label-free estimation of protein quantities was done with the Minora node implemented in Proteome Discoverer 2.4.

Metaproteome analysis

Metaproteome analysis relied on the metagenome sequences obtained from the custom metagenomics database

(see above). Annotations were refined by manual curation. All coding sequences (CDS) without codon ambiguity were compiled in one database. This database was then matched against all mass spectrometric measurements using SequestHT implemented in Proteome Discoverer 2.4 (Thermo) and results were collected. CDS containing ambiguous codons were collected in a separate database, the ambiguous positions were calculated as tryptophan and also matched against the mass spectrometric measurements. If peptides with tryptophan were later identified, they were excluded from the results. Eventually, the two result lists were merged.

Open reading frames were manually analysed regarding function and taxonomic affiliation by blast (National Library of Medicine, Bethesda, MD, USA). For functional annotation, blastp queries with predicted polypeptide sequences were used (https://blast.ncbi.nlm.nih.gov/Blast.cgi).

Cloning and sequencing of putative *nod* genes

Genomic DNA was extracted from 10 g wet weight of coarse sand using the DNeasy PowerMax Soil Kit (Qiagen) according to the manufacturer's instructions. This DNA was purified using Amicon Ultra-0.5-ml centrifugal filters (Merck) applying the protocol given by the manufacturer. The quality of the DNA was checked using a Qubit fluorometer and the Qubit dsDNA BR assay kit (Thermo Fisher Scientific). Primer combinations b: nod631F/nod1706R (amplicon size 1076 bp), d: nod684Fv2/nod1706Rv2 (amplicon size 1023 bp), and e: nod684Fv2/nod1896Rv2 (amplicon size 1213 bp) as described by Zhu et al. (2017) were used (numbering refers to the position in the *nod* gene of *Candidatus Methylomirabilis oxyfera*).

Gradient PCR was initially performed to ascertain the optimal annealing temperature with initial denaturation at 95°C for 3 min, followed by 35 cycles of 95°C for 20 s, 52 to 62°C for 20 s, 72°C for 15 s, and a final extension at 72°C for 10 min. Reaction mixtures (12.5 μl) contained 6.25 μl of MyTaq Mix 2× (BioCat), 0.7 μl (5.0 pmol) each of forward and reverse primer (oligo nucleotides synthesized by Eurofins), 1.0 μl of diluted DNA template (equivalent to 1–2 ng) and 3.85 μl nuclease free water. PCR products were checked by electrophoresis in 1.5% agarose gel applying 100 bp DNA ladder (New England Biolabs) as size standard. After electrophoresis and ethidiumbromide staining, images were obtained using the GeneTools program (Syngene).

PCR products of expected fragment size for each sample of different annealing temperatures were combined together and purified using SureClean Plus (BioCat) following the manufacturer's protocol. The purified PCR products were checked by agarose gel electrophoresis and cloned using Qiagen PCR cloning kit (Qiagen) following the manufacturer's protocol. Insert DNA of positive clones was amplified with vector-specific M13 primers, which were purified as described above and sequenced with M13 forward and reverse primers using BrilliantDye Terminator v3.1 cycle sequencing kit (Nimagen) on an ABI PRISM 3130xl Genetic Analyzer (Applied Biosystems). Assembly of contigs from forward and reverse M13 reads and trimming of vector sequences were performed using Sequencher v5.4.6 (Gene Codes). High quality sequences were compared to the NCBI nr database by blastx. DNA sequences of clones that potentially encoded NO dismutases (Nod) or NO reductases (Nor) were translated into amino acid sequences in BioEdit and aligned with Nod and Nor reference sequences using ClustalW. Neighbour-joining trees were calculated using MEGA7 software (Kumar et al., 2016).

RESULTS

Benzene mineralization under nitrate-reducing conditions

Benzene mineralization patterns were determined in microcosms incubated for up to 124 days using ^{13}C-labelled benzene as substrate and continuous analysis of increasing $\delta^{13}CO_2$ values. Benzene mineralization was dependent on the presence of nitrate and living cells and started after a lag-phase of around 50 days in all replicate cultures (Figure 1A; Figure S1; Table S1). In sacrificed triplicate microcosms, benzene was mineralized at rates of up to 28.5 ± 0.26 μM day^{-1} (day 96; Table S1; Figure S2). Based on the amount of produced $^{13}CO_2$, at least 1.2 mM benzene was mineralized by the end of the experiment out of 1.725 mM benzene added in the beginning (Table S1). Nitrite concentrations increased in the approach with labelled benzene but declined at certain time points especially around day 96 (Figure 1b). Nitrite production was also observed in the unlabelled benzene (^{12}C-benzene) approach but in lower concentrations and delayed in time (Figure 1b). Nitrite was not produced in nitrate-free, benzene-free and abiotic controls demonstrating that nitrate reduction was dependent on the simultaneous presence of benzene, living cells and added nitrate.

Changes in microbial diversity during benzene mineralization

The initial community (day 0, inoculum, solid and liquid phase) was mainly composed of *Anaerolineaceae*

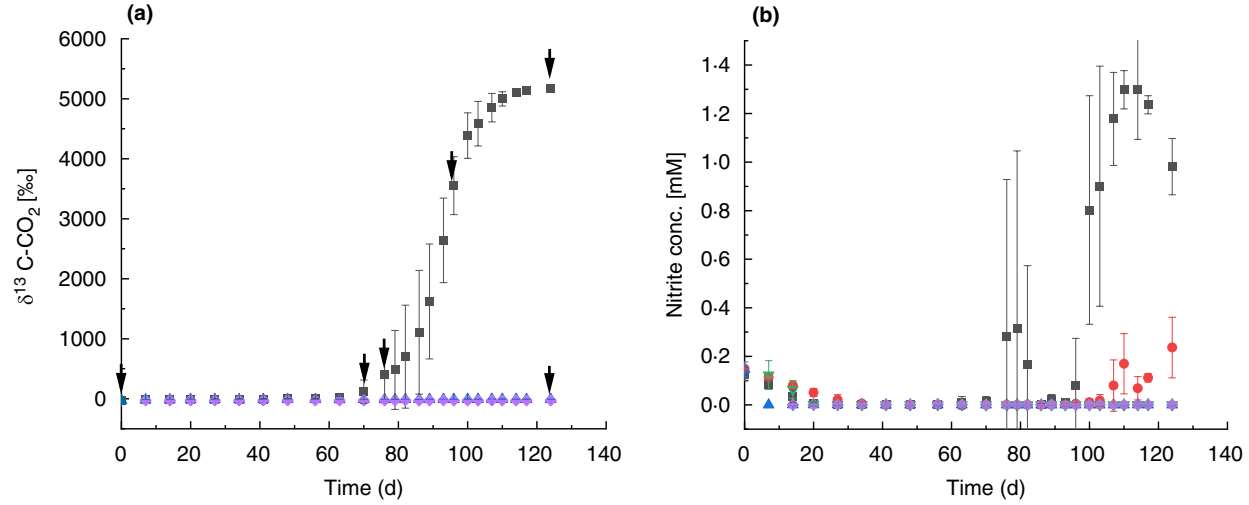

FIGURE 1 (a) Mineralization of ^{13}C-labelled benzene (25%) coupled to nitrate reduction measured by ^{13}C-CO_2 signatures, and (b) corresponding nitrite production coupled to nitrate reduction. Each data point for ^{13}C-CO_2 and nitrite is the average of all replicate cultures. Due to the stepwise sacrifice of triplicates in the course of the experiment, the number of replicates used for calculating average and standard deviation (SD) was stepwise decreasing. Black arrows indicate time points of sacrificing triplicate microcosms for metaproteomics and microbial community analysis. Grey squares: ^{13}C-benzene +nitrate; red circles: ^{12}C-benzene+nitrate; blue triangles: ^{13}C-benzene without nitrate; inverted green triangles: only nitrate; purple diamonds: ^{13}C-benzene+nitrate, sterilized

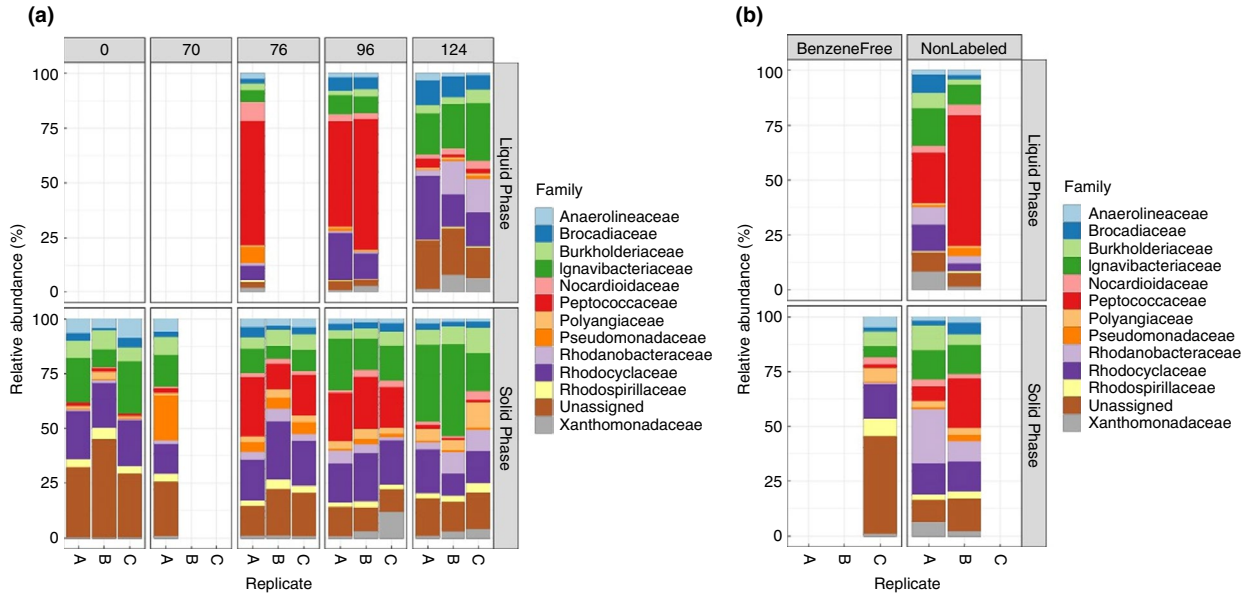

FIGURE 2 (a) Microbial community profiles upon benzene mineralization under nitrate-reducing conditions in solid and liquid phases after different times of incubation (0, 70, 76, 96, 124 days), and (b) unlabelled benzene and benzene-free approaches sampled at day 124. At each sampling time, triplicate microcosms were analysed. Blank columns represent samples of insufficient DNA amount for amplicon sequencing. Community data for 0 days in (a) include both solid and liquid phase

(4%–9%), *Brocadiaceae* (1%–4%), *Burkholderiaceae* (6%–9%), *Ignavibacteriaceae* (8%–24%), *Peptococcaceae* (1%), *Polyangiaceae* (1%–4%), *Rhodanobacteraceae* (0%–1%), *Rhodocyclaceae* (21%–22%), *Rhodospirillaceae* (3%–5%) and other unassigned taxa (Figure 2a). An ASV of the *Peptococcaceae* (Figure S3) considerably increased during benzene mineralization to 11%–27% relative abundance (day 76) and 19%–24% (day 96) in solid samples (Figure 2a), and to 57% (day 76) and up to 60% (day 96) in liquid samples (Figure 2a), suggesting a key role of this taxon for benzene assimilation. Based on comparative 16S rRNA gene sequence analyses, the *Peptococcaceae* phylotype was only distantly related to currently known anaerobic benzene-degrading *Peptococcaceae* phylotypes (Table 1). When mineralization had ceased (day 124) in the microcosms amended with ^{13}C-labelled benzene, the

TABLE 1 Closest relatives of the putative benzene-degrading *Peptococcaceae* phylotype in this study, based on BLAST identities of 16S rRNA gene sequences

Organism	Accession number	BLAST identity (%)	Source	Reference
Uncultured Peptococcaceae clone 52-03_Sulfate-G8-2[a]	HM217337	99.8	Benzene-contaminated aquifer (enriched on bactraps)	Bombach et al. (2010)
Uncultured Peptococcaceae clone 3_52_D6_b[a]	JQ087021	98.8	Benzene-contaminated aquifer (push core sediment sample)	Tischer et al. (2013)
Uncultured *Desulfosporosinus* sp. clone BEMB11B-1A1[a]	KJ955668	98.6	Bemidji core 1110 (benzene-contaminated sediment)	Beaver et al. (2016)
Uncultured bacterium clone 66_mid[a]	MF942692	98.4	Naphthalene-contaminated groundwater	Wilhelm et al. (2018)
Desulfosporosinus orientis DSM 765[b]	NR_074131	94.6	Soil at pumping station near rising main Rangoon Road (Singapore)	Pester et al. (2012)
Desulfosporosinus meridiei DSM 13257[b]	NR_074129	94.6	Groundwater contaminated with aromatic compounds	Pester et al. (2012)
Desulfitobacterium aromaticivorans UKTL[b]	NR_116427	94.6	Isolated on toluene from an iron-reducing, benzene-degrading enrichment culture	Laban et al. (2010)
Bacterium enrichment culture clone 2_71[c]	JN366539	84.5	Benzene-degrading, nitrate-reducing community enriched in a chemostat	van der Zaan et al. (2012), Atashgahi et al. (2018)
Peptococcaceae clone HS07Ba20[c]	EU016424	82.2	Benzene-degrading, iron-reducing enrichment culture	Kunapuli et al. (2007)
Peptococcaceae clone Cartwright-NO3[c]	KJ522755	82.1	Benzene-degrading, nitrate-reducing enrichment culture	Luo et al. (2014)
Uncultured *Cryptanaerobacter* clone ZZ-S9D4[c]	EF613456	81.5	Benzene-degrading, sulfate-reducing enrichment culture	Kleinsteuber et al. (2008)

[a]Most related phylotypes.

[b]Most related pure strains.

[c]Distantly related Peptococcaceae key players in anaerobic benzene-degrading enrichment cultures.

TABLE 2 Proteins related to dissimilatory inorganic nitrogen metabolism and degradation of aromatic compounds detected in this study

Serial number	Protein	Maximal score (BlastP)	Total score (BlastP)	Taxonomy (BlastP)	Sequence ID (BlastP)
1	Putative anaerobic benzene carboxylase AbcA	78.9	122	*Clostridia*	ADJ94002.1
		64.8	64.8	Uncultured bacterium (denitrifying benzene-degrading bioreactor)	QFU80959.1
2	Putative anaerobic benzene carboxylase AbcA	60.4	107	*Clostridia*	ADJ94002.1
		60.4	60.4	Uncultured bacterium (denitrifying benzene-degrading bioreactor)	QFU80959.1
3	Putative UbiX-like carboxylase, partial	67	67	*Clostridia*	ADJ94004.1
	UbiX family flavin prenyltransferase	63.5	63.5	*Desulfallas gibsoniae*	WP_006523058.1
	Hypothetical protein, partial	63.5	100	*Clostridia*	ADJ93990.1
4	6-oxocyclohex-1-ene-1-carbonyl-CoA hydratase	90.7	144	*Rhodocyclaceae*	TRZ97439.1
		90.7	149	*Rhodocyclaceae*	KAF0162674.1
5	Rieske 2Fe-2S domain-containing protein	52	52	*Modicisalibacter* sp. 'Wilcox'	WP_163647471.1
	Rieske 2Fe-2S domain-containing protein	52	52	*Halomonas* sp. A11-A	WP_110068222.1
	Alkylbenzene dioxygenase, iron sulfur protein, large subunit EbdAa	52	52	*Pseudomonas putida*	CAB99196.1
	Isopropylbenzene dioxygenase, iron-sulfur protein, large subunit	52	52	*Pseudomonas putida*	AAC03436.1
	Cumene dioxygenase alpha subunit	52	52	*Pseudomonas* sp.	ANQ47377.1
6	Hydrazine synthase subunit A, chain A	135	591	*Candidatus* Kuenenia stuttgartiensis	5C2V_A
7	Hydrazine synthase subunit A, partial	110	161	Uncultured anaerobic ammonium-oxidizing bacterium	AEW50023.1
8	Hydrazine synthase subunit A, partial	85.9	179	*Candidatus* Brocadia	AEW50029.1
9	Hydrazine synthase gamma subunit, subunit C	118	330	*Candidatus* Kuenenia stuttgartiensis	5C2V_C
10	Hydrazine synthase, subunit C	68.3	68.3	*Candidatus* Brocadia	KKO20885.1
11	Hydrazine synthase gamma subunit, partial	137	137	Uncultured anaerobic ammonium-oxidizing bacterium	AMD37564.1
12	Hydrazine synthase, partial	121	163	*Candidatus* Brocadia sp.	RIJ92455.1
13	Hydrazine dehydrogenase, partial	135	234	Uncultured anaerobic ammonium-oxidizing bacterium	AGO66620.1

TABLE 2 (Continued)

Serial number	Protein	Maximal score (BlastP)	Total score (BlastP)	Taxonomy (BlastP)	Sequence ID (BlastP)
14	Chain A, similar to hydroxylamine oxidoreductase	104	237	*Candidatus* Kuenenia stuttgartiensis	6H5L_A
15	Hydroxylamine oxidoreductase	135	234	Uncultured anaerobic ammonium-oxidizing bacterium	AGO66620.1
16	Chain A, hydroxylamine oxidoreductase	74.5	115	*Candidatus* Kuenenia stuttgartiensis	
17	Hydroxylamine oxidoreductase	59.5	154	Uncultured anaerobic ammonium-oxidizing bacterium	AXR84832.1
18	Putative hydroxylamine oxidoreductase hao	45	45	*Candidatus* Kuenenia stuttgartiensis	QII13462.1
19	Hydrazine dehydrogenase, partial	59.5	154	Uncultured anaerobic ammonium-oxidizing bacterium	AXR84832.1
20	Molybdopterin-dependent oxidoreductase	80.2	362	*Candidatus* Kuenenia stuttgartiensis	WP_164994508.1
21	Molybdopterin-dependent oxidoreductase	86.8	267	*Candidatus* Kuenenia stuttgartiensis	WP_164994508.1
22	Nitrate reductase subunit alpha, partial	50.3	50.3	*Anaerolineae*	PIV25792.1
		50.3	50.3	*Pseudonocardia ammonioxydans*	WP_093353278.1
23	Nitrite reductase	42.3	42.3	*Rhodocyclales*	OHC68864.1
				Rhodocyclales	OHC65056.1
				Betaproteobacteria	NJD33624.1
24	Cytochrome cd_1 nitrite reductase, partial	43.7	43.7	Uncultured bacterium	AHZ56215.1
25	Sec-dependent nitrous-oxide reductase	47.6	47.6	*Armatimonadetes*	HHQ53204.1
26	Sec-dependent nitrous-oxide reductase	69.6	111	*Chlorobi*	KAA0256771.1
27	Ammonia-forming cytochrome c nitrite reductase subunit c_{552}	70.4	70.4	*Chlorobi*	KAA0258279.1
28	NapC/NirT family cytochrome c	45	45	*Candidatus* Kuenenia stuttgartiensis	WP_099325822.1

Note: Sequence ID numbers are presented in the Supporting Information, TableS3.

abundance of the *Peptococcaceae* ASV decreased to low values comparable to those observed for the initial community (Figure 2). Smaller increases were observed for *Polyangiaceae* (5%–12%), *Rhodanobacteraceae* (4%–10%) and *Xanthomonadaceae* (1%–4%) in the solid phase and *Brocadiaceae* (7%–12%, only liquid samples; Figure 2a), whereas the abundances of *Brocadiaceae* (solid phase), *Ignavibacteriaceae*, and *Rhodocyclaceae* remained at roughly the same relative share. The relative abundances of *Ignavibacteriaceae* in the sediment-associated community increased to 18%–36% at day 124, resulting in a higher relative share than *Rhodocyclaceae* with 15%–20% (Figure 2a). In microcosms amended with unlabelled benzene and nitrate, *Burkholderiaceae* (2%–11%), *Ignavibacteriaceae* (9%–17%), *Rhodanobacteraceae* (3%–25%), *Rhodocyclaceae* (4%–14%) and *Peptococcaceae* (solid phase: 6%–22%; liquid phase: 23%–60%) were detected as major taxa in liquid and solid phases at day 124 (Figure 2b). The bacterial structure of other controls (nitrate-free, benzene-free and abiotic controls) was not assessed due to low DNA yields insufficient for 16S rRNA amplicon sequencing, which corresponded to the absence of benzene mineralization and associated increase of biomass in these microcosms (Figure 1a).

Metaproteome composition

Overall, 2307 peptides were detected belonging to 472 different proteins. Most proteins were assigned to the *Planctomycetes* ($n = 65$), *Chlorobi* ($n = 56$), *Betaproteobacteriales* ($n = 48$), *Chloroflexi* ($n = 31$), *Bacteroidetes* ($n = 23$) and *Firmicutes* ($n = 20$; Table 2; Table S3; Figure S4). Unclassified proteins ($n = 73$) and proteins with no identity ($n = 81$, presented as 'others', Figure S4) accounted for a substantial share of the proteins. Note that for all data shown, relative abundances of proteins are reported. A few proteins were putatively related to anaerobic degradation of aromatic compounds; notably, a subunit of the putative anaerobic benzene carboxylase AbcA and a putative UbiX-like carboxylase affiliated to the order *Clostridiales* were identified (1–3, Table 2; Table S3). Furthermore, a protein of the benzoyl-CoA downstream pathway, namely the 6-oxocyclohex-1-ene -1-carbonyl-CoA hydratase (Oah) that catalyses the ring opening transformation of 6-oxocyclohex-1-ene-1-carb onyl-CoA to 6-hydroxypimelyl-CoA, was detected and taxonomically assigned to the *Rhodocyclaceae* (4, Table 2; Table S3). Notably, also a protein affiliated to an aromatics dioxygenase was detected (5, Table 2; Table S3).

Upon incubation, AbcA was detected in various but not all solid and liquid samples taken from microcosms amended with labelled or non-labelled benzene, whereas the Oah protein was more evenly detected in the liquid and solid phase (Figure S5). A hypothetical protein with potential carboxylase function was also detected in the liquid phase (Figure S5).

With regard to dissimilatory inorganic nitrogen metabolism, proteins of the pathways for dissimilatory nitrate reduction (DNR), dissimilatory nitrate reduction to ammonium (DNRA) and anammox were identified (6–28, Table 2; Table S3). Nitrate reductase subunit alpha (NarA), nitrite reductase (Nir) associated with *Betaproteobacteria*, cytochrome cd_1 nitrite reductase (NirS), ammonia-forming cytochrome c nitrite reductase subunit c_{552} (NrfA), and various Sec-dependent nitrous-oxide reductases (NosZ) were found unevenly distributed in both liquid and solid phases over the course of the experiment (Figure S6). Nitric oxide reductase (NOR) was not found. Nir proteins were associated with Betaproteobacteria; while NrfA proteins were related to *Chlorobi* and Nos proteins were related to *Chlorobi* or *Armatimonadetes* (Table 2; Table S3; Figure S6).

With regard to anammox, hydrazine synthase subunits alpha (HzsA) and gamma (HzsG) showed high relative abundances and were consistently expressed upon incubation whereas subunit C (HzsC) was only sporadically detected (Table 2; Figure S6). Hydrazine dehydrogenase (Hdh), hydroxylamine oxidoreductases (Hao) and a molybdopterin-dependent oxidoreductase (Mop) related to typical anammox bacteria were also detected throughout the course of the experiment (13–21, Table 2; Figure S6). A NapC/NirT family cytochrome c was also found. All detected cytochrome-related proteins were of low relative abundance when compared to the relative abundances of the synthases and oxidoreductases.

Presence of putative *nod* genes

Oxygen was not detected in the liquid or in the solid phases as assessed with an additional experiment during benzene mineralization under nitrate-reducing conditions at a detection limit of 0.002% oxygen or 1 ppb (Figure S7). Amino acid sequences derived from *nod*-specific primers did not cluster with known NO dismutases but with NO reductases from *Lautropia*, *Burkholderiales* and *Microbulbifer* (Figure S8).

DISCUSSION

Putative pathways for nitrate reduction coupled with benzene mineralization

Benzene mineralization was dependent on the presence of nitrate and living cells (Figure 1a), demonstrating

that nitrate was used as the electron acceptor for benzene oxidation, also proven by the production of nitrite (Figure 1b). The observed average mineralization rates of 28.5 ± 0.3 μM day^{-1} at maximum are considerably higher than rates formerly observed under nitrate-reducing conditions in a community of similar origin (10.1 ± 1.7 μM day^{-1}; Keller et al., 2017), which might be attributed to a structural adaptation of the community to benzene as a substrate over time, thereby leading to higher mineralization rates. Benzene degradation rates between 2 and 10 μM day^{-1} were reported for other nitrate-reducing microcosm enrichment cultures (Luo et al., 2014; Toth et al., 2021).

Benzene mineralization ceased when approximately 1.2 mM of the added 1.725 mM benzene in the water/HMN phase had been mineralized (Figure 1a; Table S1), indicating that the culture was limited in inorganic nitrogen species as electron acceptors. At the beginning of the incubation, the medium was amended with 10 mM nitrate meaning that 5.8 M of nitrate were available per moles of benzene. Theoretically, benzene mineralization by nitrate reduction can result in different stoichiometry depending on the operative nitrate reduction pathway (Equations 1–3) and the simultaneous usage of reducing equivalents for the anammox reaction (Equation 4; all equations not accounting cell growth):

$$C_6H_6 + 6NO_3^- \rightarrow 6HCO_3^- + 3N_2(\text{DNR}), \quad (1)$$

$$C_6H_6 + 15NO_3^- + 3H_2O \rightarrow 6HCO_3^- + 15NO_2^- + 6H^+, \quad (2)$$

$$C_6H_6 + 3.75NO_3^- + 6.75H_2O + 1.5H^+ \rightarrow 6HCO_3^- + 3.75NH_4^+(\text{DNRA}), \quad (3)$$

$$NH_4^+ + NO_2^- \rightarrow N_2 + 2H_2O\ (\text{anammox}). \quad (4)$$

The fluctuating nitrite concentrations and the high ratio of mineralized benzene to produced nitrite strongly suggest that nitrite was not the end product of nitrate reduction (Equation 2), but further reduced by the DNR (Equation 1) or DNRA (Equation 3) pathway. For other benzene-mineralizing nitrate-reducing cultures was reported that nitrate was mainly converted to nitrite (Burland & Edwards, 1999; Luo et al., 2014; Nales et al., 1998; Ulrich & Edwards, 2003), even inhibition of benzene degradation by accumulating nitrite was observed (Burland & Edwards, 1999).

Corresponding to the observed usage of nitrate as terminal electron acceptor, we found proteins involved in canonical DNR, that is, nitrate reductase catalysing the reduction of nitrate to nitrite, and nitrite reductase converting nitrite to nitric oxide. Nitrite reduction to nitric oxide can be catalysed by a haem-containing cd1

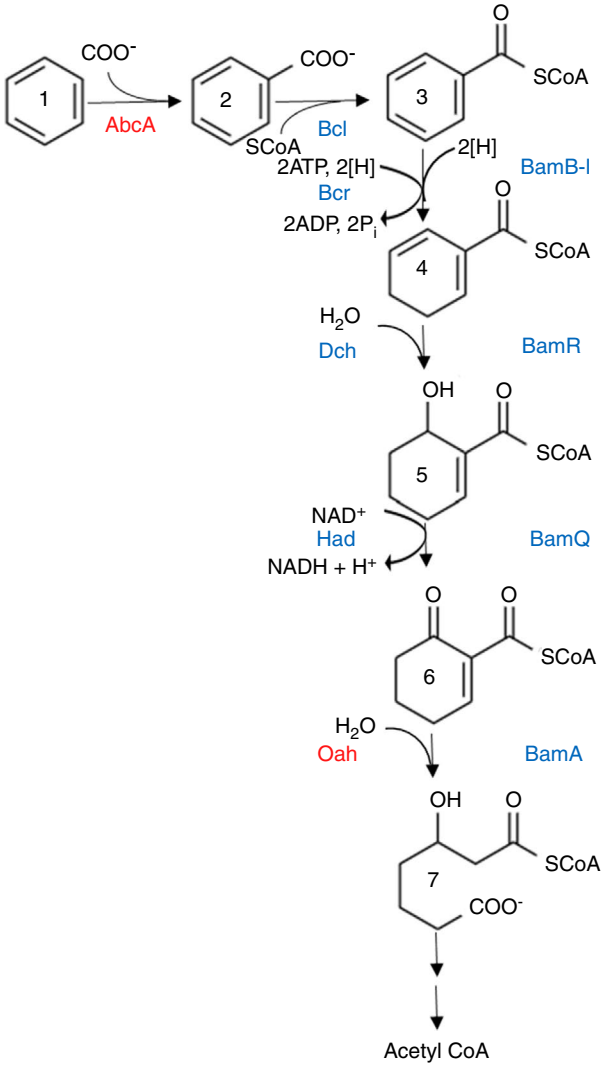

FIGURE 3 Proposed anaerobic benzene activation mechanism and downstream benzoyl-CoA transformation pathway. 1 = benzene, 2 = benzoate, 3 = benzoyl-CoA, 4 = cyclohexa-1,5-diene-1-carbonyl-CoA, 5 = 6-hydroxycyclohex-1-ene-1-carbonyl-CoA, 6 = 6-oxocyclohex-1-ene-1-carbonyl-CoA, 7 = 6-hydroxypimelyl-CoA. Proteins in red were identified in this study. AbcA, putative anaerobic benzene carboxylase subunit A; Bcl, benzoate CoA ligase; BamB-I, benzoyl-CoA reductase (class II, ATP-independent); Bcr, benzoyl-CoA reductase (class I); Dch, cyclohex-1,5-diene-1-carbonyl-CoA hydratase; Had, 6-hydroxycyclohex-1-ene-1-carbonyl-CoA hydratase; Oah, 6-oxocyclohex-1-ene-1-carbonyl-CoA hydratase

nitrite reductase (cd1-NIR, encoded by nirS) or a Cu-containing nitrite reductase (Cu-NIR, encoded by nirK), which do not contribute directly to energy conservation (Kuypers et al., 2018). We identified a cytochrome cd1 nitrite reductase, a nitrous oxide reductase transforming nitrous oxide to dinitrogen, and an ammonia-forming cytochrome c nitrite reductase (Table 2; Figure S6) indicating that both DNR and DNRA pathways were active (Equations 1 and 3).

Nitrite is also the electron acceptor for anammox (Equation 4; Kartal et al., 2013). Due to the considerable abundance of putative anammox bacteria in the microbial community (Figure 2) and the detection of high numbers of functional proteins of the anammox pathway (Table 2; Table S3), we assume that nitrite was simultaneously used as an electron acceptor for benzene and ammonium oxidation. Ammonium was available in excess (7.5 mM) in the mineral salt medium and might have been additionally produced by DNRA (Equation 3).

Elucidation of the benzene activation step

Internally produced oxygen and genes related to the *nod* gene described for *M. oxyfera*, encoding a putative oxygen-releasing dismutase, were not detected upon benzene mineralization. Cell-internal oxygenic dismutation of nitric oxide to dinitrogen and oxygen would enable microbes to employ oxygen-dependent catabolic pathways (mono- and dioxygenases) under virtually anoxic conditions. The dismutation reaction was reported to occur in the nitrate-reducing methanotrophic organism '*Ca*. *M. oxyfera*' and the alkane-oxidizing Gammaproteobacterium HdN1 (Zedelius et al., 2011). The *nod* genes encoding the putative dismutase were recovered from a range of contaminated aquifers (Zhu et al., 2017), indicating a widespread occurrence of organisms capable of oxygenic NO dismutation. The sequences we found cluster with the canonical NOR (Figure S8). Notably, we detected a protein distantly related to a Rieske dioxygenase (5, Table 2), indicating a potential for oxic benzene activation steps in the culture. However, due to the proven anoxic conditions in the microcosms, any oxic benzene-activating step would have been dependent on internally produced oxygen, a reaction which could not be verified in our study. A hydroxylation at anoxic conditions as first benzene-activation step as reported in previous studies for an iron-reducing *Geobacter* strain (Zhang et al., 2013) and methanogenic consortia (Ulrich et al., 2005; Vogel & Grbič-Galič, 1986) cannot be precluded, but remains speculative as the responsible enzyme has not been identified yet, and putative metabolites supporting this pathway were not analysed in our study.

However, we found strong indications that benzene activation and mineralization was truly anaerobic and initiated by carboxylation due to the detection of a putative benzene carboxylase, AbcA, as revealed in the metaproteome (Table 2). The detected putative AbcA was 58.6% identical to the homologous subunit of the putative benzene carboxylase identified in the *Peptococcaceae*-dominated iron-reducing benzene-degrading enrichment culture BF (Laban et al., 2010). Furthermore, we detected a UbiX-like carboxylase 64.4% similar to a putative UbiX-like carboxylase in the same benzene-degrading culture BF (Table 2). The involvement of *abc* genes related to *Peptococcaceae* in benzene carboxylation under nitrate-reducing conditions was reported in recent studies (Atashgahi et al., 2018; Luo et al., 2014; Melkonian et al., 2021; Toth et al., 2021); hence the results of these studies together with our data strongly suggest that carboxylation by *Peptococcaceae* is a common activation mechanism for benzene degradation under nitrate-reducing conditions.

Benzoyl-CoA central pathway

Benzoate is activated to benzoyl-CoA before further processing at anoxic conditions (Boll et al., 2014; Figure 3). For reduction and dearomatization of benzoyl-CoA, two pathways have been identified which are ATP-dependent or ATP-independent (Figure 3), the corresponding proteins were however not detected in the metaproteome. Notably, we identified a 6-oxocyclohex-1-ene-1-carbonyl-CoA hydratase (Oah) affiliated to *Rhodocyclaceae* (*Betaproteobacteria*), which catalyses the ring opening transformation of 6-oxocyclohex-1-ene-1-carbonyl-CoA to 6-hydroxypimelyl-CoA (Figure 3; Laempe et al., 1999), indicating that benzoyl-CoA reduction pathways have been active upon benzene metabolization.

Peptococcaceae as putative primary benzene degraders

The considerable enrichment of a partial 16S rRNA gene sequence belonging to the *Peptococcaceae* coupled to benzene mineralization suggests a key role of this organism for benzene mineralization in our culture, as already indicated by the detection of AbcA (see above). Additionally, the community structure in the labelled-benzene microcosms showed enrichment of *Brocadiaceae*, *Ignavibacteriaceae*, *Polyangiaceae*, *Rhodanobacteraceae*, *Rhodocyclaceae* and *Xanthomonadaceae* at the end of the experiment on day 124, indicating growth depending on benzene degradation and possibly syntrophic or mutualistic interactions as observed in previous studies (Atashgahi et al., 2018; Luo et al., 2014; Melkonian et al., 2021; Toth et al., 2021). *Rhodocyclaceae* and *Burkholderiaceae* were postulated as dominant benzene degraders in syntrophy with *Peptococcaceae* (Luo et al., 2014) while solely *Peptococcaceae* were implicated as responsible for activation of benzene (Atashgahi et al., 2018). The proposed syntrophic interactions in our culture need to be confirmed in future studies by, for example, reconstruction of the key player's genomes and the identification of

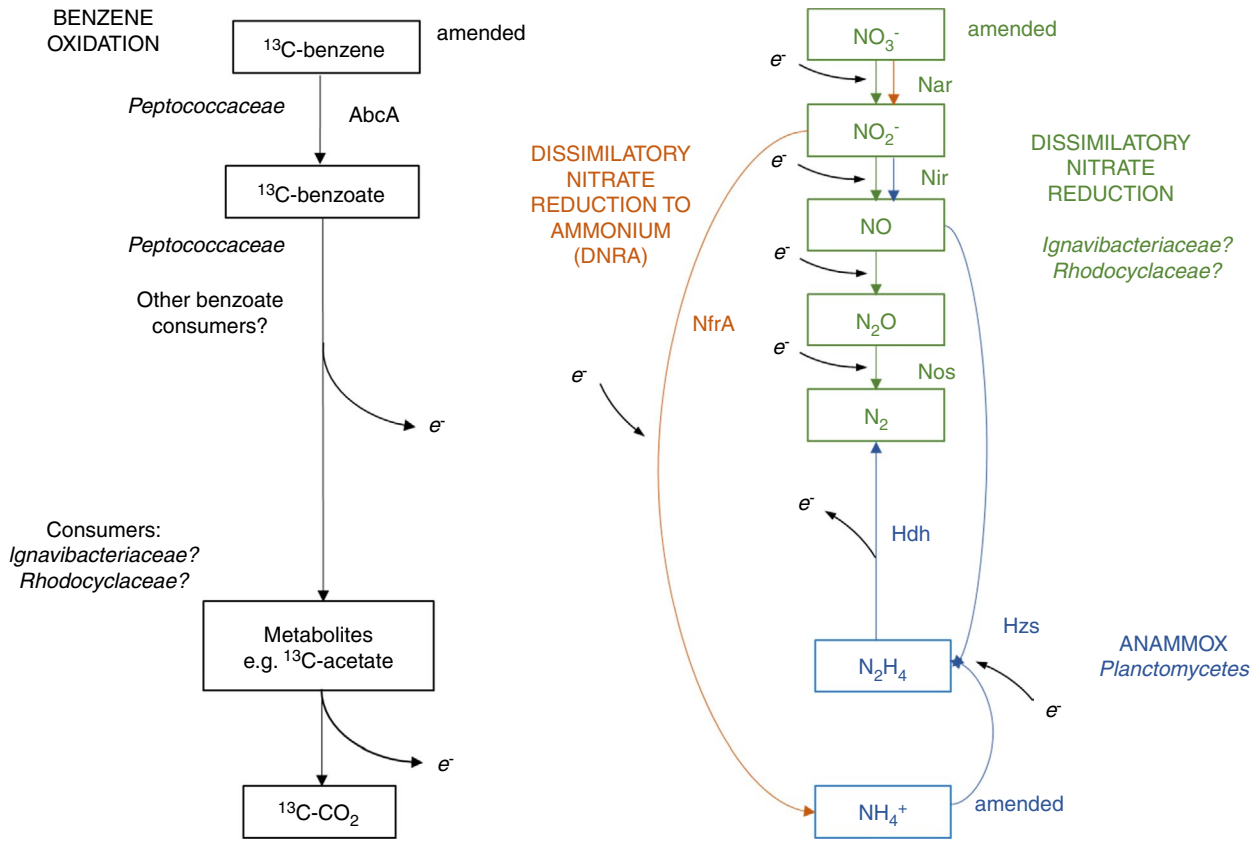

FIGURE 4 Proposed degradation pathway for benzene mineralization coupled to nitrate reduction in synergy with anammox process based on metaproteomics and microbial community analysis. Proteins indicated in black (benzene oxidation), green (DNR), orange (DNRA) and blue (anammox) were identified in the proteome analysis. AbcA, putative anaerobic benzene carboxylase; Hdh, hydrazine dehydrogenase; Hzs, hydrazine synthase subunits; Nar, nitrate reductase; NrfA, ammonia-forming cytochrome c nitrite reductase subunit c552; Nir, nitrite reductase; Nor, nitric oxide reductase

functional genes known to be involved in anaerobic benzene mineralization.

A previous study in our lab revealed *Betaproteobacteria* (*Azoarcus*, *Rhodocyclaceae*), *Ignavibacteria* and *Anaerolineae* as dominant phylotypes upon benzene degradation, whereas phylotypes related to *Peptococcaceae* and *Brocadiaceae* were absent in this consortium (Keller et al., 2017). The absence of *Brocadiaceae* in the study of Keller et al. (2017) is probably due to the usually slow growth upon anammox (Ding et al., 2018), resulting in long time periods for the enrichment of these organisms. The absence of *Peptococcaceae* in the study of Keller et al. (2017) may likely be due to the fact that the community composition was only analysed at the end of the incubation after benzene had been consumed. In this study, the *Peptococcaceae* mainly disappeared when benzene mineralization stopped, which corresponds to the observation made before (Keller et al., 2017) that *Peptococcaceae* were not detected after benzene mineralization was completed. The high abundance of *Peptococcaceae* at day 124 in the microcosms amended with non-labelled benzene (Figure 2) might be therefore due to ongoing benzene mineralization; this hypothesis is supported by the observation that production of nitrite started only after 100 days incubation in these microcosms (Figure 1b), indicating a delayed begin of benzene mineralization.

The identified *Peptococcaceae* phylotype is only distantly related to *Peptococcaceae* phylotypes detected in other benzene-mineralizing nitrate-reducing enrichment cultures (Atashgahi et al., 2018; Kunapuli et al., 2007; Luo et al., 2016; Melkonian et al., 2021; Toth et al., 2021; van der Zaan et al., 2012), and also to a *Peptococcaceae* phylotype detected as primary benzene degrader in a benzene-degrading sulfate-reducing enrichment culture isolated from the same *on-site* reactor system at the Zeitz site (Herrmann et al., 2010; Kleinsteuber et al., 2008, 2012; Taubert et al., 2012; Table 1). Benzene degrading *Peptococcaceae* may occupy distinct ecological niches depending on the used terminal electron acceptor at the Zeitz site; Peptococcaceae are typical fermenting organisms found under several electron acceptor conditions and associated with different microbial taxa (Kleinsteuber et al., 2012). Notably, the phylotype identified in our study

is closely related to a *Peptococcaceae* clone enriched in a groundwater monitoring well of the Zeitz site by *in-situ* microcosms ('bactraps') amended with benzene (Bombach et al., 2010).

Metabolic function of anammox bacteria in the community

Enrichment and activity of anammox bacteria in the community were verified by a moderate abundance of *Brocadiaceae* (7%–12%) in the liquid phase after 124 days incubation, and the detection of putative anammox-specific proteins such as hydrazine synthase, hydroxylamine oxidoreductase, hydrazine dehydrogenase and a molybdopterin-dependent oxidoreductase in the metaproteome (Table 2; Figure S6). Anammox bacteria primarily grow by the oxidation of ammonium coupled to nitrite reduction, using CO_2 as the sole carbon source (Kartal et al., 2013; Equation 4). In the microcosms, benzene degradation was coupled to nitrate reduction to nitrite and release of CO_2 while exogenous ammonium was supplied in the medium, thereby providing favourable conditions for anammox bacteria to thrive. Enrichment of anammox bacteria has previously been observed in nitrate-reducing benzene-degrading cultures (Atashgahi et al., 2018; Han et al., 2020; Luo et al., 2014; Melkonian et al., 2021; Peng et al., 2017) and also a nitrate-reducing cyclohexane-degrading enrichment culture (Musat et al., 2010), and some of these studies revealed that the presence of anammox bacteria can increase nitrate-dependent benzene degradation rates indicating anammox bacteria might detoxify nitrite (Han et al., 2020; Peng et al., 2017). Yang et al. (2019) established that nitrite is a common substrate of anammox and denitrification processes, which affects nitrogen removal performance. Thus, denitrifying and anammox bacteria may be co-occurring in our system to regulate nitrite concentrations. This effect could be useful in nitrogen compound removal in natural environments, however, the loss of electron acceptor capacity due to reduction of nitrite by anammox bacteria could be a disadvantage for some remediation strategies. The proposed denitrification pathway in our enrichment culture in combination with the anammox metabolic pathway is shown in Figure 4.

In summary, benzene was mineralized anoxically under nitrate-reducing conditions. Microbial community analyses indicated that a distinct member of the *Peptococcaceae* was growing while oxidizing benzene and other members of the community became also slightly enriched suggesting that benzene was mineralized by syntrophic interactions of the primary benzene degrader with nitrate reducers. Similar communities have been reported by others (Atashgahi et al., 2018; Kunapuli et al., 2007; Luo et al., 2016; Melkonian et al., 2021), but the initial degrader observed in this study is phylogenetically distinct from other putative benzene degraders indicating a broad diversity of anaerobic benzene degraders within the *Peptococcaceae*. In addition, benzene was likely initially carboxylated as indicated by metaproteomic detection of subunit AbcA of the putative benzene carboxylase; this protein has always been detected in benzene-degrading *Peptococcaceae*-dominated cultures to date. Identified anammox bacteria may support nitrate-dependent benzene mineralization by consuming the potentially toxic nitrite. The observed changes in microbial composition highlight complex interactions among the different taxa.

ACKNOWLEDGEMENT

This work was supported by the German Academic Exchange Service (DAAD) funding SCE, the Helmholtz Association (Germany) through the Young Investigator Group [VH-NG-1248] funding UNR and FBC, and the European regional development funds (EFRE—Europe Funds Saxony) plus the Helmholtz Association. Open access funding enabled and organized by ProjektDEAL.

CONFLICT OF INTEREST

The authors declare no conflict of interest.

ORCID

Samuel C. Eziuzor https://orcid.org/0000-0002-5488-6834
Carsten Vogt https://orcid.org/0000-0002-7605-6356

REFERENCES

Atashgahi, S., Hornung, B., Van Der Waals, M.J., Da Rocha, U.N., Hugenholtz, F., Nijsse, B. et al. (2018) A benzene-degrading nitrate-reducing microbial consortium displays aerobic and anaerobic benzene degradation pathways. *Scientific Reports*, 8, 4490. https://doi.org/10.1038/s41598-018-22617-x

Bayliss, D.L., Chen, C., Sonawane, B. & Valcovic, L. (1998) Carcinogenic effects of benzene: an update. EPA/600/P-97/001A 1–43

Beaver, C.L., Williams, A.E., Atekwana, E.A., Mewafy, F.M., Abdel Aal, G., Slater, L.D. et al. (2016) Microbial communities associated with zones of elevated magnetic susceptibility in hydrocarbon-contaminated sediments. *Geomicrobiology Journal*, 33(5), 441–452. https://doi.org/10.1080/01490451.2015.1049676

Boll, M., Löffler, C., Morris, B.E.L. & Kung, J.W. (2014) Anaerobic degradation of homocyclic aromatic compounds via arylcarboxyl-coenzyme A esters: organisms, strategies and key enzymes. *Environmental Microbiology*, 16(3), 612–627. https://doi.org/10.1111/1462-2920.12328

Bolyen, E., Rideout, J.R., Dillon, M.R., Bokulich, N.A., Abnet, C.C., Al-Ghalith, G.A. et al. (2019) Reproducible, interactive, scalable and extensible microbiome data science using QIIME 2.

Nature Biotechnology, 37(8), 852–857. https://doi.org/10.1038/s41587-019-0209-9

Bombach, P., Hübschmann, T., Fetzer, I., Kleinsteuber, S., Geyer, R., Harms, H. et al. (2010) Resolution of natural microbial community dynamics by community fingerprinting, flow cytometry, and trend interpretation analysis. *Advances in Biochemical Engineering/Biotechnology*, 124, 151–181. https://doi.org/10.1007/10_2010_82

Burland, S.M. & Edwards, E.A. (1999) Anaerobic benzene biodegradation linked to nitrate reduction. *Applied and Environment Microbiology*, 65, 529–533. https://doi.org/10.1128/aem.65.2.529-533.1999

Callahan, B.J., McMurdie, P.J., Rosen, M.J., Han, A.W., Johnson, A.J.A. & Holmes, S.P. (2016) DADA2: high-resolution sample inference from Illumina amplicon data. *Nature Methods*, 13(7), 581–583. https://doi.org/10.1038/nmeth.3869

Coates, J.D., Chakraborty, R., Lack, J.G., O'Connor, S.M., Cole, K.A., Bender, K.S. et al. (2001) Anaerobic benzene oxidation coupled to nitrate reduction in pure cultures by two strains of *Dechloromonas*. *Nature*, 411, 1039–1043. https://doi.org/10.1038/35082545

Coplen, T.B. (2011) Guidelines and recommended terms for expression of stable-isotope-ratio and gas-ratio measurement results. *Rapid Communications in Mass Spectrometry*, 25(17), 2538–2560. https://doi.org/10.1002/rcm.5129

Díaz, E., Jiménez, J.I. & Nogales, J. (2013) Aerobic degradation of aromatic compounds. *Current Opinion in Biotechnology*, 24, 431–442.

Ding, C., Enyi, F.O. & Adrian, L. (2018) Anaerobic ammonium oxidation (Anammox) with planktonic cells in a redox-stable semicontinuous stirred-tank reactor. *Environmental Science & Technology*, 52, 5671–5681.

Ettwig, K.F., Butler, M.K., Le Paslier, D., Pelletier, E., Mangenot, S., Kuypers, M.M.M. et al. (2010) Nitrite-driven anaerobic methane oxidation by oxygenic bacteria. *Nature*, 464, 543–548. https://doi.org/10.1038/nature08883

European Chemicals Agency (ECHA) (1998) ANNEX 1. Background Document in Support of the Committee for Risk Assessment (RAC) Evaluation of Limit Values for Benzene in the Workplace. Helsinki. ECHA/RAC/A77-0-0000001412-86-187/F.

Fuchs, G. (2008) Anaerobic degradation of aromatic compounds. *Annals of the New York Academy of Sciences*, 1125, 82–99. https://doi.org/10.1196/annals.1419.010

Han, X., Peng, S., Zhang, L., Lu, P. & Zhang, D. (2020) The co-occurrence of DNRA and Anammox during the anaerobic degradation of benzene under denitrification. *Chemosphere*, 247, 125968. https://doi.org/10.1016/j.chemosphere.2020.125968

Herrmann, S., Kleinsteuber, S., Chatzinotas, A., Kuppardt, S., Lueders, T., Richnow, H.H. et al. (2010) Functional characterization of an anaerobic benzene-degrading enrichment culture by DNA stable isotope probing. *Environmental Microbiology*, 12, 401–411. https://doi.org/10.1111/j.1462-2920.2009.02077.x

Holmes, D.E., Risso, C., Smith, J.A. & Lovley, D.R. (2011) Anaerobic oxidation of benzene by the hyperthermophilic archaeon *Ferroglobus placidus*. *Applied and Environment Microbiology*, 77(17), 5926–5933. https://doi.org/10.1128/AEM.05452-11

Kartal, B., de Almeida, N.M., Maalcke, W.J., Op den Camp, H.J.M., Jetten, M.S.M. & Keltjens, J.T. (2013) How to make a living from anaerobic ammonium oxidation. *FEMS Microbiology Reviews*, 37, 428–461. https://doi.org/10.1111/1574-6976.12014

Kasai, Y., Takahata, Y., Manefield, M. & Watanabe, K. (2006) RNA-based stable isotope probing and isolation of anaerobic benzene-degrading bacteria from gasoline-contaminated groundwater. *Applied and Environment Microbiology*, 72(5), 3586–3592. https://doi.org/10.1128/AEM.72.5.3586-3592.2006

Keller, A.H., Kleinsteuber, S. & Vogt, C. (2017) Anaerobic benzene mineralization by nitrate-reducing and sulfate-reducing microbial consortia enriched from the same site: comparison of community composition and degradation characteristics. *Microbial Ecology*, 75(4), 941–953. https://doi.org/10.1007/s00248-017-1111-y

Kleinsteuber, S., Schleinitz, K.M., Breitfeld, J., Harms, H., Richnow, H.H. & Vogt, C. (2008) Molecular characterization of bacterial communities mineralizing benzene under sulfate-reducing conditions. *FEMS Microbiology Ecology*, 66, 143–157. https://doi.org/10.1111/j.1574-6941.2008.00536.x

Kleinsteuber, S., Schleinitz, K.M. & Vogt, C. (2012) Key players and team play: anaerobic microbial communities in hydrocarbon-contaminated aquifers. *Applied Microbiology and Biotechnology*, 94, 851–873. https://doi.org/10.1007/s00253-012-4025-0

Klindworth, A., Pruesse, E., Schweer, T., Peplies, J., Quast, C., Horn, M. et al. (2013) Evaluation of general 16S ribosomal RNA gene PCR primers for classical and next-generation sequencing-based diversity studies. *Nucleic Acids Research*, 41(1), 1–11. https://doi.org/10.1093/nar/gks808

Kumar, S., Stecher, G. & Tamura, K. (2016) MEGA7: molecular evolutionary genetics analysis version 7.0 for Bigger Datasets. *Molecular Biology and Evolution*, 33(7), 1870–1874. https://doi.org/10.1093/molbev/msw054

Kunapuli, U., Lueders, T. & Meckenstock, R.U. (2007) The use of stable isotope probing to identify key iron-reducing microorganisms involved in anaerobic benzene degradation. *The ISME Journal*, 1, 643–653. https://doi.org/10.1038/ismej.2007.73

Kuypers, M.M.M., Marchant, H.K. & Kartal, B. (2018) The microbial nitrogen-cycling network. *Nature Reviews Microbiology*, 16(5), 263–276. https://doi.org/10.1038/nrmicro.2018.9

Laban, N.A., Selesi, D., Rattei, T., Tischler, P. & Meckenstock, R.U. (2010) Identification of enzymes involved in anaerobic benzene degradation by a strictly anaerobic iron-reducing enrichment culture. *Environmental Microbiology*, 12, 2783–2796. https://doi.org/10.1111/j.1462-2920.2010.02248.x

Laempe, D., Jahn, M. & Fuchs, G. (1999) 6-Hydroxycyclohex-1-ene-1-carbonyl-CoA dehydrogenase and 6-oxocyclohex-1-ene-1-carbonyl-CoA hydrolase, enzymes of the benzoyl-CoA pathway of anaerobic aromatic metabolism in the denitrifying bacterium *Thauera aromatica*. *European Journal of Biochemistry*, 263(2), 420–429. https://doi.org/10.1046/j.1432-1327.1999.00504.x

Landon, M.K. & Belitz, K. (2012) Geogenic sources of benzene in aquifers used for public supply, California. *Environmental Science and Technology*, 46, 8689–8697. https://doi.org/10.1021/es302024c

Luo, F., Devine, C.E. & Edwards, E.A. (2016) Cultivating microbial dark matter in benzene-degrading methanogenic consortia. *Environmental Microbiology*, 18(9), 2923–2936. https://doi.org/10.1111/1462-2920.13121

Luo, F., Gitiafroz, R., Devine, C.E., Gong, Y., Hug, L.A., Raskin, L. et al. (2014) Metatranscriptome of an anaerobic benzene-degrading, nitrate-reducing enrichment culture reveals involvement of carboxylation in benzene ring activation. *Applied*

and Environment Microbiology, 80(14), 4095–4107. https://doi.org/10.1128/AEM.00717-14

McMurdie, P.J. & Holmes, S. (2013) Phyloseq: an R package for reproducible interactive analysis and graphics of microbiome census data. *PLoS One*, 8(4), e61217. https://doi.org/10.1371/journal.pone.0061217

Melkonian, C., Fillinger, L., Atashgahi, S., da Rocha, U.N., Kuiper, E., Olivier, B. et al. (2021) High biodiversity in a benzene-degrading nitrate-reducing culture is sustained by a few primary consumers. *Communications Biology*, 4(1), 530. https://doi.org/10.1038/s42003-021-01948-y

Meyer, F., Paarmann, D., D'Souza, M., Olson, R., Glass, E.M., Kubal, M. et al. (2008) The metagenomics RAST server—a public resource for the automatic phylogenetic and functional analysis of metagenomes. *BMC Bioinformatics*, 9, 1–8. https://doi.org/10.1186/1471-2105-9-386

Musat, F., Wilkes, H., Behrends, A., Woebken, D. & Widdel, F. (2010) Microbial nitrate-dependent cyclohexane degradation coupled with anaerobic ammonium oxidation. *The ISME Journal*, 4(10), 1290–1301. https://doi.org/10.1038/ismej.2010.50

Nales, M., Butler, B.J. & Edwards, E.A. (1998) Anaerobic benzene biodegradation: a microcosm survey. *Bioremediation Journal*, 2, 125–144.

Peng, S., Zhang, L., Zhang, D.J., Lu, P., Zhang, X. & He, Q. (2017) Denitrification synergized with anammox for the anaerobic degradation of benzene: performance and microbial community structure. *Applied Microbiology and Biotechnology*, 101(10), 4315–4325. https://doi.org/10.1007/s00253-017-8166-z

Perez-Riverol, Y., Csordas, A., Bai, J., Bernal-Llinares, M., Hewapathirana, S., Kundu, D.J. et al. (2019) The PRIDE database and related tools and resources in 2019: improving support for quantification data. *Nucleic Acids Research*, 47(D1), D442–D450.

Pester, M., Brambilla, E., Alazard, D., Rattei, T., Weinmaier, T., Han, J. et al. (2012) Complete genome sequences of *Desulfosporosinus orientis* DSM765T, *Desulfosporosinus youngiae* DSM17734T, *Desulfosporosinus meridiei* DSM13257T, and *Desulfosporosinus acidiphilus* DSM22704T. *Journal of Bacteriology*, 194(22), 6300–6301. https://doi.org/10.1128/JB.01392-12

Quast, C., Pruesse, E., Yilmaz, P., Gerken, J., Schweer, T., Yarza, P. et al. (2013) The SILVA ribosomal RNA gene database project: improved data processing and web-based tools. *Nucleic Acids Research*, 41(D1), D590–D596. https://doi.org/10.1093/nar/gks1219

Raihan, S., Ahmed, N., Macaskie, L.E. & Lloyd, J.R. (1997) Immobilisation of whole bacterial cells for anaerobic biotransformations. *Applied Microbiology and Biotechnology*, 47(4), 352–357. https://doi.org/10.1007/s002530050939

Rajeev, L., Nunes da Rocha, U., Klitgord, N., Luning, E.G., Fortney, J., Axen, S.D. et al. (2013) Dynamic cynobacterial response to hydration and dehydration in a desert biological soil crust. *The ISME Journal*, 7, 2178–2191. https://doi.org/10.1038/ismej.2013.83

Rakoczy, J., Schleinitz, K.M., Muller, N., Richnow, H.H. & Vogt, C. (2011) Effects of hydrogen and acetate on benzene mineralisation under sulfate-reducing conditions. *FEMS Microbiology Ecology*, 77, 238–247. https://doi.org/10.1111/j.1574-6941.2011.01101.x

Taubert, M., Vogt, C., Wubet, T., Kleinsteuber, S., Tarkka, M.T., Harms, H. et al. (2012) Protein-SIP enables time-resolved analysis of the carbon flux in a sulfate-reducing, benzene-degrading microbial consortium. *The ISME Journal*, 6(12), 2291–2301. https://doi.org/10.1038/ismej.2012.68

Tischer, K., Kleinsteuber, S., Schleinitz, K.M., Fetzer, I., Spott, O., Stange, F. et al. (2013) Microbial communities along biogeochemical gradients in a hydrocarbon-contaminated aquifer. *Environmental Microbiology*, 15(9), 2603–2615. https://doi.org/10.1111/1462-2920.12168

Toth, C.R.A., Luo, F., Bawa, N., Webb, J., Guo, S., Dworatzek, S. et al. (2021) Anaerobic benzene biodegradation linked to the growth of highly specific bacterial clades. *Environmental Science & Technology*, 55, 7970–7980. https://doi.org/10.1021/acs.est.1c00508

Türkowsky, D., Lohmann, P., Mühlenbrink, M., Schubert, T., Adrian, L., Goris, T. et al. (2019) Thermal proteome profiling allows quantitative assessment of interactions between tetrachloroethene reductive dehalogenase and trichloroethene. *Journal of Proteomics*, 192, 10–17. https://doi.org/10.1016/j.jprot.2018.05.018

Ulrich, A.C., Beller, H.R. & Edwards, E.A. (2005) Metabolites detected during biodegradation of $^{13}C_6$-benzene in nitrate-reducing and methanogenic enrichment cultures. *Environmental Science and Technology*, 39, 6681–6691. https://doi.org/10.1021/es050294u

Ulrich, A.C. & Edwards, E.A. (2003) Physiological and molecular characterization of anaerobic benzene degrading mixed cultures. *Environmental Microbiology*, 5, 92–102.

van der Zaan, B.M., Saia, F.T., Stams, A.J.M., Plugge, C.M., de Vos, W.M., Smidt, H. et al. (2012) Anaerobic benzene degradation under denitrifying conditions: *Peptococcaceae* as dominant benzene degraders and evidence for a syntrophic process. *Environmental Microbiology*, 14(5), 1171–1181. https://doi.org/10.1111/j.1462-2920.2012.02697.x

Vogel, T.M. & Gribič-Galič, D. (1986) Incorporation of oxygen from water into toluene and benzene during anaerobic fermentative transformation. *Applied and Environment Microbiology*, 52, 200–202.

Vogt, C., Godeke, S., Treutler, H.C., Weiss, H., Schirmer, M. & Richnow, H.H. (2007) Benzene oxidation under sulfate-reducing conditions in columns simulating in situ conditions. *Biodegradation*, 18, 625–636. https://doi.org/10.1007/s10532-006-9095-1

Vogt, C., Kleinsteuber, S. & Richnow, H.H. (2011) Anaerobic benzene degradation by bacteria. *Microbial Biotechnology*, 4, 710–724. https://doi.org/10.1111/j.1751-7915.2011.00260.x

Weelink Sander A. B., van Eekert Miriam H. A., Stams Alfons J. M. (2010) Degradation of BTEX by anaerobic bacteria: physiology and application. *Reviews in Environmental Science and Biotechnology*, 9, (4), 359. –385. http://dx.doi.org/10.1007/s11157-010-9219-2

Wilhelm, R.C., Hanson, B.T., Chandra, S. & Madsen, E. (2018) Community dynamics and functional characteristics of naphthalene-degrading populations in contaminated surface sediments and hypoxic/anoxic groundwater. *Environmental Microbiology*, 20(10), 3543–3559. https://doi.org/10.1111/1462-2920.14309

Yang, J., Li, J., Zheng, Z., Hou, L., Liang, D., Sun, Y. et al. (2019) Effect of organic matters on anammox coupled denitrification system: when nitrite was sufficient. *Royal Society Open Science*, 6(11), 11159. https://doi.org/10.1098/rsos.190771

Zedelius, J., Rabus, R., Grundmann, O., Werner, I., Brodkorb, D., Schreiber, F. et al. (2011) Alkane degradation under

anoxic conditions by a nitrate-reducing bacterium with possible involvement of the electron acceptor in substrate activation. *Environmental Microbiology Reports*, 3(1), 125–135. https://doi.org/10.1111/j.1758-2229.2010.00198.x

Zhang, T., Tremblay, P.L., Chaurasia, A.K., Smith, J.A., Bain, T.S. & Lovley, D.R. (2013) Anaerobic benzene oxidation via phenol in *Geobacter metallireducens*. *Applied and Environment Microbiology*, 79(24), 7800–7806. https://doi.org/10.1128/AEM.03134-13

Zhu, B., Bradford, L., Huang, S., Szalay, A., Leix, C., Weissbach, M. et al. (2017) Unexpected diversity and high abundance of putative nitric oxide dismutase (Nod) genes in contaminated aquifers and wastewater treatment systems. *Applied and Environment Microbiology*, 83(4), 1–13. https://doi.org/10.1128/AEM.02750-16

SUPPORTING INFORMATION

Additional supporting information may be found in the online version of the article at the publisher's website.

How to cite this article: Eziuzor, S.C., Corrêa, F.B., Peng, S., Schultz, J., Kleinsteuber, S., da Rocha, U.N., et al. (2022) Structure and functional capacity of a benzene-mineralizing, nitrate-reducing microbial community. *Journal of Applied Microbiology*, 00, 1–17. https://doi.org/10.1111/jam.15443